Progress in Oceanography xxx (xxxx) xxx–xxx

Contents lists available at ScienceDirect

Progress in Oceanography

journal homepage: www.elsevier.com/locate/pocean

Growth and mortality of coccolithophores during spring in a temperate Shelf Sea (Celtic Sea, April 2015)

K.M.J. Mayers[a,*], A.J. Poulton[b,1], C.J. Daniels[b], S.R. Wells[c], E.M.S. Woodward[d], G.A. Tarran[d], C.E. Widdicombe[d], D.J. Mayor[b], A. Atkinson[d], S.L.C. Giering[b]

[a] Ocean and Earth Science, National Oceanography Centre Southampton, University of Southampton, Southampton, UK
[b] National Oceanography Centre, Waterfront Campus, European Way, Southampton, UK
[c] Institute of Biological and Environmental Sciences, University of Aberdeen, Oceanlab, Newburgh, Aberdeenshire, UK
[d] Plymouth Marine Laboratory, Prospect Place, The Hoe, Plymouth, UK

ARTICLE INFO

Keywords:
Coccolithophores
Growth rates
Microzooplankton grazing
Calcite production
Dissolution
Spring bloom

ABSTRACT

Coccolithophores are key components of phytoplankton communities, exerting a critical impact on the global carbon cycle and the Earth's climate through the production of coccoliths made of calcium carbonate (calcite) and bioactive gases. Microzooplankton grazing is an important mortality factor in coccolithophore blooms, however little is currently known regarding the mortality (or growth) rates within non-bloom populations. Measurements of coccolithophore calcite production (CP) and dilution experiments to determine microzooplankton (≤63 μm) grazing rates were made during a spring cruise (April 2015) at the Central Celtic Sea (CCS), shelf edge (CS2), and within an adjacent April bloom of the coccolithophore *Emiliania huxleyi* at station J2.

CP at CCS ranged from 10.4 to 40.4 μmol C m^{-3} d^{-1} and peaked at the height of the spring phytoplankton bloom (peak chlorophyll-*a* concentrations ~6 mg m^{-3}). Cell normalised calcification rates declined from ~1.7 to ~0.2 pmol C $cell^{-1}$ d^{-1}, accompanied by a shift from a mixed coccolithophore species community to one dominated by the more lightly calcified species *E. huxleyi* and *Calciopappus caudatus*. At the CCS, coccolithophore abundance increased from 6 to 94 cells mL^{-1}, with net growth rates ranging from 0.06 to 0.21 d^{-1} from the 4th to the 28th April. Estimates of intrinsic growth and grazing rates from dilution experiments, at the CCS ranged from 0.01 to 0.86 d^{-1} and from 0.01 to 1.32 d^{-1}, respectively, which resulted in variable net growth rates during April. Microzooplankton grazers consumed 59 to > 100% of daily calcite production at the CCS. Within the *E. huxleyi* bloom a maximum density of 1986 cells mL^{-1} was recorded, along with CP rates of 6000 μmol C m^{-3} d^{-1} and an intrinsic growth rate of 0.29 d^{-1}, with ~80% of daily calcite production being consumed.

Our results show that microzooplankton can exert strong top-down control on both bloom and non-bloom coccolithophore populations, grazing over 60% of daily growth (and calcite production). The fate of consumed calcite is unclear, but may be lost either through dissolution in acidic food vacuoles, and subsequent release as CO_2, or export to the seabed after incorporation into small faecal pellets. With such high microzooplankton-mediated mortality losses, the fate of grazed calcite is clearly a high priority research direction.

1. Introduction

Coccolithophores are a diverse and biogeochemically important group of marine phytoplankton which contribute towards the marine carbon cycle through the production and subsequent export of cellular scales (coccoliths) formed of calcium carbonate (calcite). The cellular process of calcite production (calcification) fixes and releases CO_2 and hence coccolithophores have an important role in air-sea CO_2 fluxes (e.g. Holligan et al., 1993; Buitenhuis et al., 1996). Calcite can also act as a ballast for sinking material, enhancing the deep-sea flux of organic matter (Bach et al., 2016; Klaas and Archer, 2002; Ziveri et al., 2007). Coccolithophores are globally distributed, from polar to tropical low-latitude waters, with the most cosmopolitan and abundant species being *Emiliania huxleyi* (e.g. Winter and Siesser, 1994). *E. huxleyi* often forms extensive, large-scale (> 100,000 km^2) blooms in the open ocean (e.g. Holligan et al., 1993), along continental shelves (e.g. Holligan

* Corresponding author.
E-mail address: kyle.mayers@soton.ac.uk (K.M.J. Mayers).
[1] Current address: The Lyell Centre, Heriot-Watt University, Edinburgh, UK.

https://doi.org/10.1016/j.pocean.2018.02.024

et al., 1983; Poulton et al., 2013) and in coastal shelf seas (e.g. Buitenhuis et al., 1996; Krueger-Hadfield et al., 2014; Rees et al., 2002).

Phytoplankton blooms are common in shelf sea environments during late spring, when environmental conditions allow growth to exceed mortality and biomass to accumulate. The community structure within these blooms may change with time as environmental conditions such as nutrient and light availability favour one phytoplankton group over another. Coccolithophore blooms are considered to be favoured under conditions between high-turbulence high-nutrient and low-turbulence low-nutrient environments (Balch, 2004). However, satellite-derived particulate inorganic calcite and chlorophyll-*a* data from open ocean regions suggest that blooms of coccolithophores can also co-occur with blooms of other phytoplankton (e.g. diatoms), and sequential succession between groups may not always occur (Hopkins et al., 2015). In situ observations made during several phytoplankton blooms support the co-occurrence of coccolithophores with other groups, including diatoms and dinoflagellates in both open ocean and coastal environments (see Daniels et al., 2015; Poulton et al., 2013, 2014; Schiebel et al., 2011), however we currently lack in situ data from shelf sea environments during spring.

Blooms of *E. huxleyi* have been shown to be important sources of calcite production (CP) (e.g. Balch et al., 2005; Poulton et al., 2007, 2013), primary production (PP) (up to 30–40% (Poulton et al., 2013)), CO_2 fluxes (e.g. Buitenhuis et al., 1996), and the production of the bioactive gas dimethyl sulphide (e.g. Malin et al., 1993). Within some shelf sea regions, *E. huxleyi* blooms are an annual feature (e.g. English Channel, Patagonian Shelf) whereas in others they appear sporadically though, recently at an increased frequency (e.g. Barent's Sea, Black Sea) (Iglesias-Rodriguez et al., 2002; Smyth et al., 2004). How these blooms fit into global budgets of CP is currently unclear, though they are localised sites of high CP and export (Holligan et al., 1993; Poulton et al., 2013).

The formation of *E. huxleyi* blooms, which often occur in late summer, is thought to be linked to several environmental factors including; warm, stratified waters, with low silicic acid concentrations (limiting diatoms), high irradiance, low nitrate to phosphate ratios, and reduced microzooplankton grazing (see review by Tyrrell and Merico, 2004). Microzooplankton (< 200 μm) are major grazers of phytoplankton, consuming from 49% to 77% of daily PP (Schmoker et al., 2013). The relationship between coccolithophores and microzooplankton grazing is currently unclear as only a few studies, most of which during coccolithophore blooms, have investigated microzooplankton-induced coccolithophore mortality. A study carried out during an *E. huxleyi* bloom in the Bering Sea found lower grazing rates within bloom waters than outside bloom waters, which led to higher net growth rates compared with outside of the bloom (Olson and Strom, 2002). A similar result was observed in the English Channel (Fileman et al., 2002), suggesting depressed grazing rates on coccolithophores could be a trigger for bloom formation and persistence.

At the cellular scale, calcification accounts for ~30% of photosynthetically fixed energy and hence represents a important fraction of the total cellular metabolism available for key cellular processes such as nutrient uptake and cell division (Monteiro et al., 2016). The ecological or physiological role of calcification is not fully known, though several hypotheses exist, such as protection from light stress, enhancement of photosynthesis, buoyancy regulation and as a protection from grazing (Young, 1994; Monteiro et al., 2016). A recent modelling study proposed that calcification has different ecological roles across different oceanic provinces (Monteiro et al., 2016). However, experimental results have so far demonstrated less clarity on the role of calcification. For example, culture experiments with the heterotrophic dinoflagellate *Oxyrrhis marina* showed grazing to be higher on calcified *E. huxleyi* cells than naked ones (Hansen et al., 1996). More recently, another culture experiment has shown that grazing rates on *E. huxleyi* appeared to be dependent on the strain studied rather than cell calcite content, although the growth rates of the heterotrophic dinoflagellates and their overall grazing impact were depressed due to the cellular degree of calcification (Harvey et al., 2015).

The aim of our study was to examine the variability in the rates at which coccolithophore communities grow and are being grazed on by microzooplankton, and how these relate to environmental conditions and the microzooplankton community. We carried out our study during April, as this is the key period in temperate shelf seas for the spring phytoplankton bloom and not generally associated with coccolithophore blooms which typically occur in late summer. We measured coccolithophore growth and mortality rates, alongside observations of coccolithophore species composition and CP, during April at three sites in the Celtic Sea in order to examine: (1) the role of coccolithophores in carbon cycling during spring, (2) coccolithophore growth rates during the spring bloom, and (3) the role of microzooplankton grazing in coccolithophore population dynamics.

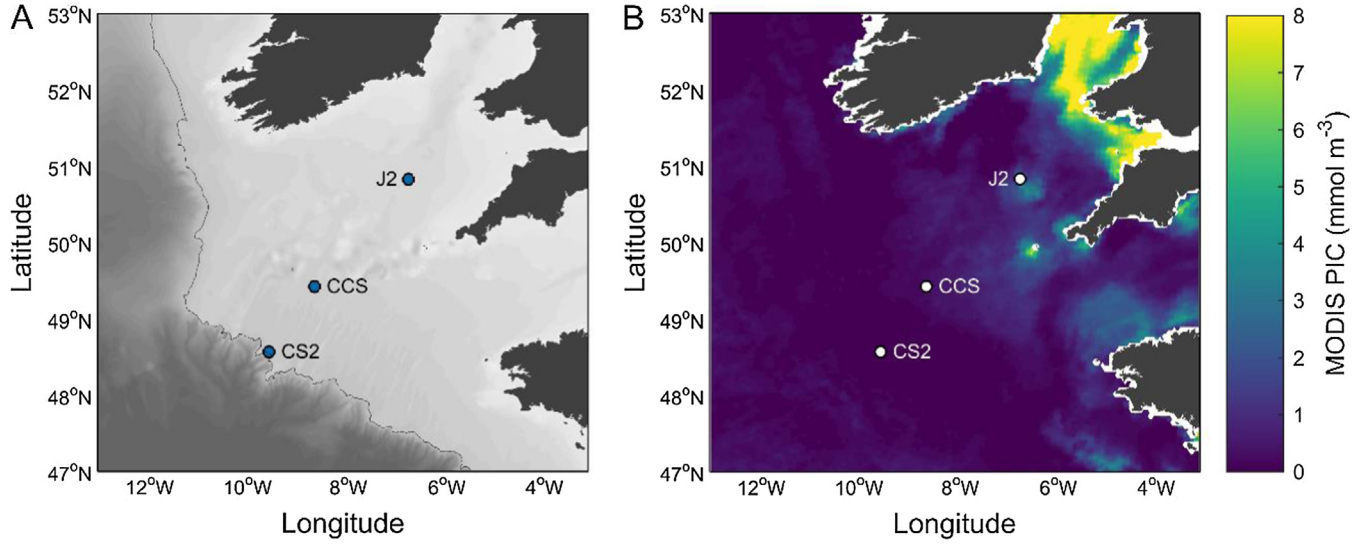

Fig. 1. Sampling locations within the Celtic Sea superimposed onto depth (left) with dark colours corresponding to deep waters and MODIS particulate inorganic carbon (PIC) concentration for April 2015. Central Celtic Sea (CCS), Shelf Edge (CS2), and station J2.

2. Methods

2.1. Study site

Sampling was carried out on-board the *RRS Discovery* (cruise number DY029) from 1st April to 29th April 2015 in the Celtic Sea (Fig. 1; NW European Shelf) as part of the UK Shelf Sea Biogeochemistry (SSB) research programme. Water sampling was carried out at 10 pre-dawn stations (02:00–03:30 h GMT) using a conductivity-temperature-depth (CTD) profiler with rosette sampler fitted with twenty-four 20 L Niskin bottles. Seawater samples were obtained from six light depths within the upper 100 m, determined as 60, 40, 20, 10, 5 and 1% of surface irradiance (see Poulton et al., this issue for full methodology) for rate measurements (primary production (PP), calcite production (CP)), phytoplankton biomass (chlorophyll-*a*) and coccolithophore community structure. The main sampling stations in this study were the Central Celtic Sea (CCS; 150 m water depth), the Celtic Shelf Edge (CS2; 203 m water depth) and station J2 (Fig. 1). Throughout this paper, the term 'spring bloom' is used to refer to a peak in chlorophyll-*a* biomass ($\sim$6 mg m^{-3}; see Sharples et al., this issue) in the middle (15th) of April at CCS, and 'coccolithophore bloom' to refer to the high cellular coccolithophore abundances at J2.

2.2. Nutrients and chlorophyll measurements

Water samples for determination of nutrient concentrations (nitrate + nitrite, nitrite, phosphate, and silicic acid) were collected directly from the CTD into aged, acid-washed and Milli-Q-rinsed 60 mL HDPE Nalgene™ bottles. Clean sampling and handling techniques were employed during the sampling and manipulations within the laboratory, and where possible carried out according to the International GO-SHIP nutrient manual recommendations (Hydes et al., 2010). Nutrient samples were all analysed on board the *RRS Discovery* using a Bran and Luebbe segmented flow colorimetric auto-analyser using techniques described in Woodward and Rees (2001). Nutrient reference materials (KANSO Japan) were run each day to check analyser performance and to guarantee the quality control of the final reported data. The typical uncertainty of the analytical results were between 2 and 3%, and the limits of detection for nitrate and phosphate was 0.02 μmol L^{-1}, nitrite 0.01 μmol L^{-1}, whilst silicic acid was always higher than the limits of detection. Further details of the nutrient analysis and seasonal variability in nutrient inventories can be found in Humphreys et al. (this issue).

Water samples (0.2–0.25 L) for chlorophyll-*a* extraction were filtered onto 25 mm diameter Whatman GF/F or Fisherbrand MF300 glass fibre filters (effective pore sizes 0.7 μm) and extracted in 6–10 mL 90% acetone (HPLC grade, Sigma-Aldrich, UK) at −4°C for 18–24 h (Poulton et al., 2014). Fluorescence was measured on a Turner Designs Trilogy fluorometer using a non-acidification module and calibrated with a solid standard and a pure chlorophyll-*a* standard (Sigma-Aldrich, UK).

2.3. Coccolithophore community enumeration and composition

Samples for coccolithophore cell counts and community composition were sampled as described by Poulton et al. (2010). Briefly, samples were collected from the six light depths, seawater samples (0.2–0.5 L) were filtered under gentle pressure through 25-mm diameter, 0.8-μm pore size Nuclepore™ cellulose nitrate filters with a Whatman GF/F backing filter to aid in equal distribution of material across the filter. Filters were rinsed with trace ammonia solution (pH ~ 10–11), oven dried for ~12 h at 50–60 °C and stored in Millipore petri-slides. Permanent slides of the filters were prepared on board by mounting the filters using low viscosity Norland Optical Adhesive 074 (Poulton et al., 2010). Samples were analysed under cross-polarized light using an Olympus BX51 (x1000, oil immersion). Either 300 individual cells or 300 fields of view (whichever was reached first) were counted per sample with a minimum number of 50 fields of view being counted. Cell numbers (cells mL^{-1}) were calculated based on the area of filter examined (total area of filtered material divided by the number of fields of view multiplied by area of 1 field of view), cells counted and volume filtered (mL). Full coccospheres were identified following the taxonomy of Frada et al. (2010) to the lowest possible taxonomic unit. Standard errors in cell counts were calculated using Eq. (1):

$$\frac{(\sqrt{C})}{(FOV \times \frac{V}{A})} \quad (1)$$

where C is the number of cells counted, A is the area investigated (mm^2), FOV is the number of field of views counted and V is the volume of water filtered (mL) (Taylor, 1982).

For a small number of samples (usually taken at the depth of 40% surface irradiance) further species identification and cell counts were carried out using scanning electron microscopy (SEM) following Young et al. (2003) to identify species. Coccolithophore community diversity was determined and expressed as species richness (total number of species in a sample, S) and Pielou's evenness (J′), which is a measure of how evenly distributed species are in a community (high values represent dominance by a one or a few species). J′ was calculated as described by Charalampopoulou et al., (2011, 2016).

2.4. Primary production and coccolithophore calcification rates

Daily rates (24 h from dawn to dawn) of primary production (PP) and calcite production (CP) were determined for each of the 10 stations sampled using the methodology described by Balch et al. (2000) (see also Poulton et al., 2010, 2013, 2014). Seawater samples were collected before dawn (02:00–03:00 local time), and subsamples from the six light depths decanted into four 70 mL polycarbonate (Corning™) flasks: 3 light replicates and 1 formalin-killed control. All samples were spiked with 34 to 44 μCi of ^{14}C-labelled sodium bicarbonate and placed in dedicated incubation chambers with a combination of LED light panels (Powerpax, UK) and neutral density light filters (Lee Filters™, UK) to replicate the absolute daily light doses at the depths of collection (see Poulton et al., this issue). Formalin killed blanks were prepared by adding 1 mL of 0.2-μm filtered borate-buffered formalin solution.

Incubations were ended by filtering through polycarbonate filters (25-mm diameter, 0.4-μm nominal pore size, Nuclepore™, USA), with extensive rinsing to remove unfixed ^{14}C-labelled sodium bicarbonate. Organic (PP) and inorganic (CP) carbon fixation were determined using the micro-diffusion technique (Paasche and Brutak, 1994; Balch et al., 2000; Poulton et al., 2014), the filters were then placed in fresh glass scintillation vials with 12 mL of Ultima Gold™ (Perkin-Elmer, UK) liquid scintillation cocktail added. The activity on the filters was then determined using a Tri-Carb 3100TR Liquid Scintillation Counter on-board. The spike activity was checked by the removal of triplicate 100 μL subsamples directly after the spike addition and mixing with 200 μL of β-phenylethylamine (Sigma, UK) followed by Ultima Gold™ and liquid scintillation counting (Poulton et al., 2014). The average coefficient of variation (standard deviation/mean × 100) of triplicate PP measurements was 13% (1–59%) and 47% (1–143%) for CP measurements. The formalin-killed blank represented 27% (< 1–600%) of the CP signal on average, with higher contributions observed at the base of the euphotic zone.

2.5. Coccolithophore net growth rates

Net growth rates of coccolithophores were determined from 24 h incubations. Water was collected before dawn as described above. Water samples (250 mL) from the 40% incident irradiance depth were taken directly from the CTD. Three samples were filtered immediately (T_0 counts), whilst three more samples were placed in a dedicated incubation chamber (as described above; see also Poulton et al., this

issue) for 24 hrs, and then filtered. Samples were filtered under gentle vacuum through cellulose nitrate filters (25 mm diameter, 0.8 μm pore size Nuclepore™) with a Whatman GF/F backing filter to aid in equal distribution of material across the filter. Filters were treated as discussed above and coccospheres identified. Net growth rates (μ, d^{-1}) of coccolithophores were determined using Eq. (2):

$$\mu = \left(\frac{1}{t}\right) LN \left(\frac{n24}{n0}\right) \quad (2)$$

where t is time in days, n_{24} is the number of cells mL^{-1} at the end of the incubations and n_0 the number of cells mL^{-1} taken directly from the CTD.

2.6. Coccolithophore growth and microzooplankton grazing

Daily rates of coccolithophore growth and mortality were estimated using the dilution technique (Landry and Hassett, 1982; Landry et al., 1995). Seawater samples from the upper mixed layer (5–10 m water depth) were collected in 10 L acid-clean carboys and passed through a 63 μm mesh to exclude larger zooplankton. Use of a 63 μm mesh in this study was aimed at excluding larger grazers and focusing on grazing by microzooplankton on coccolithophores and phytoplankton ≤63 μm. A proportion of the seawater was filtered through 0.2 μm cartridge filters using gravitational filtration. Sequential dilutions were made of 100, 70, 40 and 20% ambient seawater. Samples were gently agitated prior to sampling to ensure they were well mixed. Nutrients were not added to incubation bottles as there is evidence this may impact on microzooplankton abundance (Gifford, 1988) and phytoplankton growth (Lessard and Murrell, 1998). Furthermore, nutrient levels (nitrate, phosphate, silicate) remained in replete concentrations throughout most of the sampling period (> 2 μmol kg^{-1} for nitrate and silicate, and > 100 nmol kg^{-1} for phosphate; see Humphreys et al., this issue; Poulton et al., this issue). During the entire setting up procedure, seawater was kept in a temperature-controlled laboratory set to in situ temperatures (± 2 °C), and was handled in near darkness to minimise exposure to light.

Samples for nutrients, coccolithophores (by cell counts, see Section 2.3), microzooplankton (by FlowCAM, see below) and chlorophyll-*a* (see Section 2.2), were taken for initial measurements from 63 μm screened water. Twelve 3 L glass jars were filled with the seawater dilutions (triplicates of each dilution), sealed without a bubble present, and incubated for 24 h in a controlled temperature (CT) refrigeration container (see Richier et al., 2014; Poulton et al., this issue). After 24 h, the samples were removed from the incubators and the same suite of measurements taken as for the initial measurements (cell counts, microzooplankton abundance, chlorophyll-a), ensuring samples were mixed before sub-sampling. For coccolithophore cell abundances, 250 mL of seawater was filtered through a 0.8 μm pore size Nuclepore™ cellulose nitrate filters with a Whatman GF/F backing filter to aid in equal distribution of material across the filter, filters were then treated the same as for CTD samples (see Section 2.2).

Growth rates were calculated as in Eq. (2). Changes in coccolithophore cell numbers, measured by cross-polarized light microscopy (see Section 2.2) were used to calculate apparent growth rates, assuming:

$$NGR = k - cg = \frac{1}{t} LN \left(\frac{Pt}{Po}\right) \quad (3)$$

where P_0 and P_t are the initial and final cell numbers, k is the intrinsic growth rate of coccolithophores (Y-intercept), g is the coefficient of grazing mortality (the slope of the linear regression) and c is the dilution factor (1, 0.7, 0.4, and 0.2) (Landry and Hassett, 1982; Landry et al., 1995). Two main assumptions of the dilution technique are that phytoplankton growth rates are unaffected by dilution, and that the rate of grazing mortality is proportional to the dilution impact on grazer abundance (Landry and Hassett, 1982; Landry et al., 1995).

We calculated the percentage of daily growth consumed by microzooplankton as intrinsic growth rate (μ) divided by the coefficient of grazing mortality (g). As we will be discussing the consumption of calcite-bearing phytoplankton, we also refer to this as the fraction of calcite production consumed per day rather than primary production.

2.7. Microzooplankton abundance

Sub-samples (10–20 mL) of preserved microzooplankton in acidic Lugol's Iodine (2% final concentration) collected at T0 and T24 from dilution experiments were analysed using FlowCAM VS-IVc (Fluid Imaging Technologies Inc.) fitted with a 300 μm path length flow cell and x4 microscope objective. Images were collected using auto-image mode at a rate of 6–12 frames per second. Image files were manually classified to determine the abundance of dinoflagellates and ciliates using Visual spreadsheet software (Version 3.2.3).

2.8. Statistical analysis

All statistical analyses were carried out in SigmaPlot (v12.5). Growth rate errors for incubation experiments were calculated using error propagation and linear regressions. An F-test was used to look for differences in the linear regressions within dilution experiments for total coccolithophore communities and *E. huxleyi*.

3. Results

3.1. General oceanography

Samples were taken during April 2015 at the three sites in the Celtic Sea: Central Celtic Sea (CCS), the shelf edge (CS2), and a shallower station (J2) (Fig. 1). Throughout April, CCS was more frequently sampled (n = 5) than CS2 (n = 2) and J2 (n = 2). Hydrographic conditions varied during spring at CCS, with sea surface temperature varying from 9.8 °C to 11.2 °C and mixed layer depth (MLD) (determined as an increase of 0.01 kg m^{-3} from the potential density at 10 m; Hopkins, pers. comms) shoaling from 51 m at the beginning of April to 16 m by the end of the month. The shelf-break (CS2) showed slightly higher temperatures than CCS with little variability between subsequent visits (11.4–11.8 °C) and a small decrease in MLD from 27 m to 24 m. The shallower J2 site had sea surface temperatures between 9.8 °C and 10.4 °C and a slightly shallower MLD than CS2 (20–22 m; Table 1). Poulton et al. (this issue) gives details of the seasonal variability in absolute irradiance across the euphotic zone.

Surface nitrate (NOx) and phosphate decreased throughout April from 6 to 0.4 μmol kg^{-1} and 0.5 to 0.1 μmol kg^{-1}, respectively, at CCS (Table 1). Between each subsequent visit to CCS, NOx declined, apart from between the 15th and 20th April (1.4–2.0 μmol kg^{-1}), which coincided with a slight drop in sea surface temperature (11.1–10.8 °C) and likely indicates a mixing event, though there was no noticeable change in MLD (25–24 m). At J2, NOx was also drawn down between subsequent visits (4.2–0.6 μmol kg^{-1}), though only to a limited degree at CS2 (8.2–6.1 μM). The same pattern was observed for phosphate at J2 (0.4–0.1 μM) and CS2 (0.5–0.4 μM). Silicic acid remained relatively high at all stations during spring, ranging from 3.5 to 2.2 μmol kg^{-1}, with an April average of 2.7 (± 0.4) μmol kg^{-1}. At both CCS and CS2, ammonia concentrations increased from less than 0.1 to ~0.2 μmol kg^{-1}, but showed a larger increase at J2 from 0.1 to 0.4 μmol kg^{-1} (Table 1).

Integrated euphotic zone chlorophyll-*a* ranged from 35.2 to 132.1 mg m^{-2} in the Celtic Sea during spring, with the highest values found at the CCS on 15th April and the lowest at the shelf edge (CS2) on the 10th April (Table 2). At CCS, from 4th to 15th April, euphotic zone integrated chlorophyll-*a* concentrations increased 3-fold, associated with a 4-fold increase in PP (Table 2). At CS2, euphotic zone integrated chlorophyll-*a* increased from 35.2 to 59.8 mg m^{-2} between visits and had a higher integrated PP (81.1–155.1 mmol C m^{-2}) (Table 2). J2 was

Table 1
Environmental conditions for calcification and coccolithophore cell experiments conducted in the Celtic Sea during April 2015. Euphotic depth was determined during the cruise to be the depth of 1% photosynthetically active radiation (PAR). Not determined (ND).

			Surface macronutrients						
Sampling sites	Day in April	SST (°C)	NO^3 (μM)	PO^4 (μM)	$Si(OH)^4$ (μM)	NH^4 (μM)	N:P ratio	Euphotic depth (m)	Mixed layer depth (m)
CCS	4	9.8	6.0	0.5	2.8	< 0.1	12	37	51
CCS	6	10	5.6	0.4	2.7	< 0. <	14	37	47
CCS	11	10.3	3.8	0.3	2.6	0.1	13	32	22
CCS	15	11.1	1.4	0.2	2.6	0.1	7	28	25
CCS	20	10.8	2.0	0.2	2.4	0.2	10	28	24
CCS	25	11.2	0.4	0.1	2.2	0.2	4	35	16
CS2	10	11.4	8.2	0.5	3.1	< 0.1	16	48	27
CS2	24	11.8	6.1	0.4	2.3	0.2	15	30	24
J2	14	9.8	4.2	0.4	3.5	0.1	11	ND	20
J2	27	10.4	0.6	0.1	2.9	0.4	6	ND	22
Mean			3.8	0.3	2.7	0.2	11	34	28
Min			0.4	0.1	2.2	< 0.1	4	28	16
Max			8.2	0.5	3.5	0.4	16	48	51

the site of an *Emiliania huxleyi* bloom on 27th April, however sampling on the 14th April found higher chlorophyll-*a* (121.4 and 45.2 mg m^{-2}, respectively). Euphotic zone integrated PP was much higher during the *E. huxleyi* bloom than on the 14th April (524.2 and 112.3 mg m^{-2}, respectively) (Table 2).

3.2. Coccolithophore abundances and species composition

Measurements of upper euphotic zone (60, 40 and 20% PAR light depths) coccolithophore cell abundance at CCS ranged from 7.6 to 91 cells mL^{-1}, with a positive trend observed throughout April (Fig. 2b). Over the entire euphotic zone, average coccolithophore abundance also continually increased at CCS throughout April (6.3–96 cells mL^{-1}) (Fig. 3). The first visit to J2 on the 14th April showed high cell numbers (155.6 cells mL^{-1}), which had increased to 1986 cells mL^{-1} (*E. huxleyi*) cells 13 days later on the 27th April (Table 3).

At CCS the coccolithophore community was dominated (> 49% by abundance) by *E. huxleyi*, with this dominance becoming more pronounced later in April (up to 76%) (Table 3). Increasing *E. huxleyi* dominance coincided with an increase in the relative abundance of the coccolithophore *Calciopappus caudatus*. (5–26%) and a decline in "other" species (34–2%) (Table 3), such as the larger coccolithophore *Coronosphaera mediterranea* (7 to < 1%). This trend is also seen in Pielou's evenness (J') which declined from 0.7 to 0.4, as well as species richness (the number of different species present) which declined from 11 to 6, with lowest values observed on the 25th April. The shelf-edge site CS2 was also dominated by *E. huxleyi*, however this site showed a lower abundance of *C. caudatus*. (10–2%) and a higher abundance of other species (30–42%), which coincided with high values of J′ (0.5–0.6) and species richness (9–10). At J2, the community was almost exclusively (99%) *E. huxleyi*, with J′ and species richness both extremely low during both visits to this site (0.1–0 and 2–1, respectively). Morphotype A of *E. huxleyi* (after Young et al., 2003) dominated the J2 bloom and was the common morphotype throughout the spring bloom at the CCS in April (see Supplementary Figure 1).

Discrete measurements of coccolithophore cell numbers within the Celtic Sea ranged from 3.4 (± 0.1) to 150.5 (± 2.2) cells mL^{-1} (Fig. 3), with the abundance patterns showing good agreement with average euphotic zone cell numbers (Table 3). Maximum cell numbers at CCS were found below the 60% incidental irradiance depth at all sites, though there was variability in the depth where this maximum occurred. For example, at CCS on the 11th and 25th April maximum cell numbers appeared to coincide with the MLD (Fig. 3).

3.3. Calcite production and primary production

Rates of calcite production (CP) sampled at discrete depths within the euphotic zone ranged from 0.7 to 81.3 μmol C m^{-3} d^{-1} at CCS and from 2.4 to 65.2 μmol C m^{-3} d^{-1} at CS2 (Fig. 3). Vertical profiles of CP (Fig. 3) consistently showed minimum values at the base of the euphotic zone and maximum rates in the upper euphotic zone (aside from a maximum at 15 m at CCS on 20th April). There also appeared to be a

Table 2
Euphotic zone integrated measurements of chlorophyll-*a*, primary production and calcite production.

		Chlorophyll-*a*			Primary and calcite production			
Sampling sites	Day in April	Total Chl *a* (mg m^{-2})	2–20 μm fraction (%)	Coccolithophore contribution (%)[a]	PP (mmol C m^{-2})	Coccolithophore contribution (%)	CP (mmol C m^{-2})	CP:PP ratio
CCS	4	46.8	58	0.1	101.7	0.3	0.4	< 0.01
CCS	6	57.8	53	0.1	54.4	0.7	0.4	0.01
CCS	11	102.6	67	0.2	137.3	0.3	0.5	< 0.01
CCS	15	132.1	91	0.2	435.1	0.2	1.0	< 0.01
CCS	20	105.2	73	0.5	220.6	0.3	0.7	< 0.01
CCS	25	112.2	64	0.6	326.9	0.2	0.7	< 0.01
CS2	10	35.2	46	1.0	81.1	1.8	1.5	0.02
CS2	24	59.8	72	1.4	155.1	0.7	1.1	0.01
J2	14	121.4	67	1.0	112.3	8.6	10.6	0.09
J2	27	45.2	69	18.8	524.2	30.6	239.8	0.46
Mean		81.8	66	2.4	214.9	4.4	25.7	0.1
Min.		35.2	46	0.1	54.4	0.2	0.4	< 0.01
Max.		132.1	91	18.8	524.2	30.6	239.8	0.46

[a] Calculated based on the assumption all coccolithophores were *E. huxleyi* and contained 0.34 pg chl-a $cell^{-1}$ (Daniels et al., 2014).

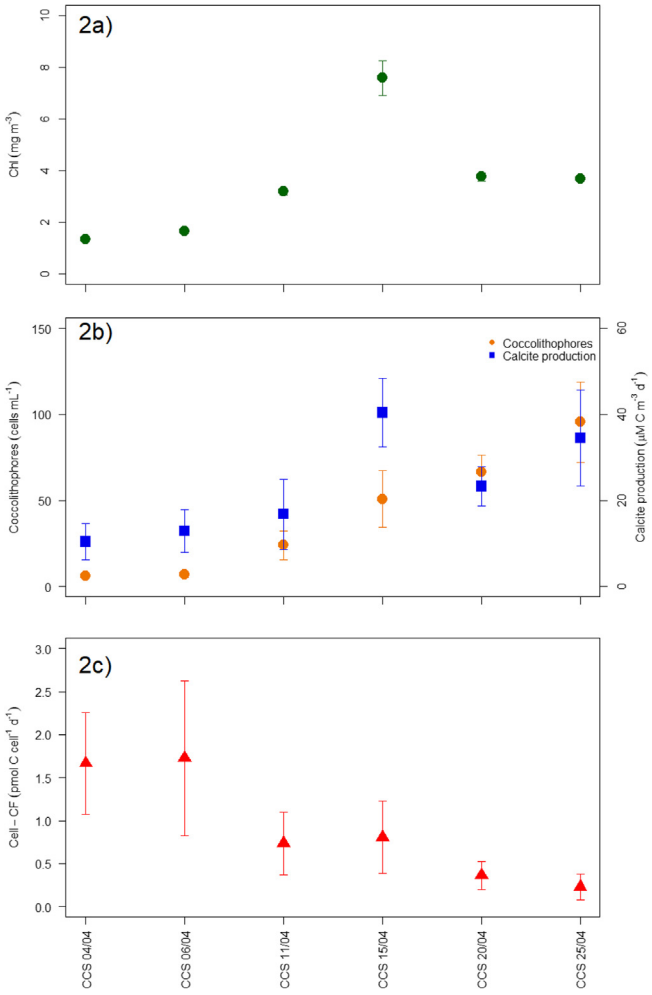

Fig. 2. Average chlorophyll-*a* (mg m^{-2}) (2a), coccolithophore cell numbers (circles, cell mL^{-1}) and calcite production (squares, µmol C $m^{-3}d^{-1}$) (2b) and cell normalised calcification rates (2c), over the top 3 light depths (60, 40 and 20% photosynthetically active radiation) at the Central Celtic Sea (CCS). Error bars show ± 1 standard deviation.

declining trend in CP with depth in association with decreasing irradiance, with this decline seen below the MLD (Fig. 3). Euphotic zone integrated CP at CCS varied from 0.4 to 1 mmol C m^{-2} d^{-1}, with a ratio of CP to PP consistently less than 0.01 (Table 2). At station J2, integrated euphotic zone CP was consistently higher (14th April, 10.6 mmol C m^{-2} d^{-1}; 27th April, 239.8 mmol C m^{-2} d^{-1}) with CP: PP ratios of 0.09 and 0.46, respectively (Table 2). Integrated CP showed a similar peak to integrated chlorophyll-*a* on the 15th April (Fig. 2b). Normalising CP to coccolithophore cell numbers, to give cell specific CP (Cell-CF; Poulton et al., 2010; Table 3, Fig. 2c), showed high values at the CCS during the beginning of April (2.0–2.5 pmol C $cell^{-1}$ d^{-1}), which declined throughout April to reach a minimum of ~0.4 pmol C $cell^{-1}$ d^{-1} on the 25th (Fig. 2c).

Euphotic zone integrated PP showed a similar temporal trend to integrated chlorophyll-*a* and CP. Integrated PP at CCS ranged from 54.4 to 435.1 mmol C m^{-2} d^{-1}, with the peak on the 15th April, the same date as the highest chlorophyll-*a* biomass (Table 2). Overall, integrated PP was highest on the 27th April at the site of the *E. huxleyi* bloom (J2; 524.2 mmol C m^{-2} d^{-1}), which was a five-fold increase from earlier measurements on the 14th April (112.3 mmol C m^{-2} d^{-1}). In contrast to CCS and J2, CS2 had comparatively low integrated PP throughout April (81.1–155.1 mmol C $m^{-2}d^{-1}$).

3.4. Net growth rate comparison

Net coccolithophore growth experiments were conducted four times at CCS and once at station J2 on the 27th April for 24 h from the 40% PAR depth. On the 11th April net growth rates (NGR) were 0.31 d^{-1} (Table 4). On the 15th April coccolithophore NGRs were negative (−0.15 d^{-1}), and positive on both the 20th April (0.16 d^{-1}) and the 25th April (0.20 d^{-1}). During the *E. huxleyi* bloom at J2, coccolithophore NGRs were observed as 0.11 d^{-1} (Table 4). We can also calculate the net growth rates between subsequent visits to CCS, CS2 and J2 (Table 3). At CCS, net growth rates of 0.04 d^{-1} were observed in early April, ~0.2 d^{-1} on the 11th and 15th April and 0.06 d^{-1} at the end of April. At J2 a net growth rate of 0.2 d^{-1} was observed between the 14 and 27 April. This calculation does not take into account advective processes, which likely impacts coccolithophore populations.

3.5. Growth and mortality rates from dilution experiments

Based on dilution experiments conducted during April all regression slopes were found to be significantly different from zero ($p \leq 0.02$) (Fig. 5), apart from on the 4th April at CCS and on the 9th April at CS2, with all other dilution experiments showing a good correlation coefficient for the linear regression ($R^2 \geq 0.44$) (Table 5). From all experiments, a positive slope was only encountered at CCS on the 20th April (Fig. 5), whilst all others were negative. Due to the negative growth rate also found on 20th April (−0.39 d^{-1}), and the violation to the assumptions of the dilution technique (Landry et al., 1995; Landry and Hassett, 1982), we will not comment on this result further. The lack of nutrient addition within the experiments did not appear to negatively impact coccolithophore growth rates, even during late April experiments (see Supplementary Fig. 2).

Intrinsic (gross) growth rates were variable during spring at CCS (0.0–1.2 d^{-1}) with an initial increase on the 11th April (0.86 d^{-1}), declining on the 15th April (0.36 d^{-1}) and finally peaking again on the 25th April (1.2 d^{-1}). Grazing rates of microzooplankton (≤63 µm; due to mesh screening) showed a positive trend throughout spring at CCS, ranging from 0.1 to 1.3 d^{-1} (Table 5). The percentage of calcite production consumed in the Celtic Sea ranged from 59 to > 100%, with the lowest observed on the 11th April and the highest on the 15th April. Results were not statistically different (F-test) between *E. huxleyi* and total coccolithophores for either intrinsic growth ($p = 0.21$) or mortality ($p = 0.46$) rates, likely due to *E. huxleyi* dominating cell abundances (Table 3). The dilution experiment from the 27th April at J2 (*E. huxleyi* bloom) displayed an intrinsic growth rate of 0.29 d^{-1} and a grazing coefficient of 0.23 d^{-1} (Table 5), demonstrating high (79%) microzooplankton grazing mortality during this coccolithophore bloom event.

Microzooplankton abundances (dinoflagellates and ciliates) were determined for all T0 experiments (apart from 20 April) whilst T24 abundances were determined for all aside from experiments conducted on 15 and 20 April (Table 6). Abundances of microzooplankton at T0 at the CCS declined from 1610(± 335) to 280(± 160) cells L^{-1} and were 190(± 120) and 460(± 58) cells L^{-1} at the shelf edge and station J2 respectively (Table 6). Ciliates and dinoflagellates represented on average 44(± 13) and 56(± 13) % of the total abundance in the dilution experiments. The growth rates of ciliates in experiments varied between −0.35 and 1.6 d^{-1}, showing higher values later in April (Table 6). The same trend is observed for dinoflagellates, with growth rates between −0.34 and 1.7 d^{-1}.

4. Discussion

4.1. Coccolithophores during spring in the Celtic Sea

Coccolithophores were present at all of the sites sampled within the Celtic Sea during spring. By assuming a chlorophyll-*a* content of 0.34 pg

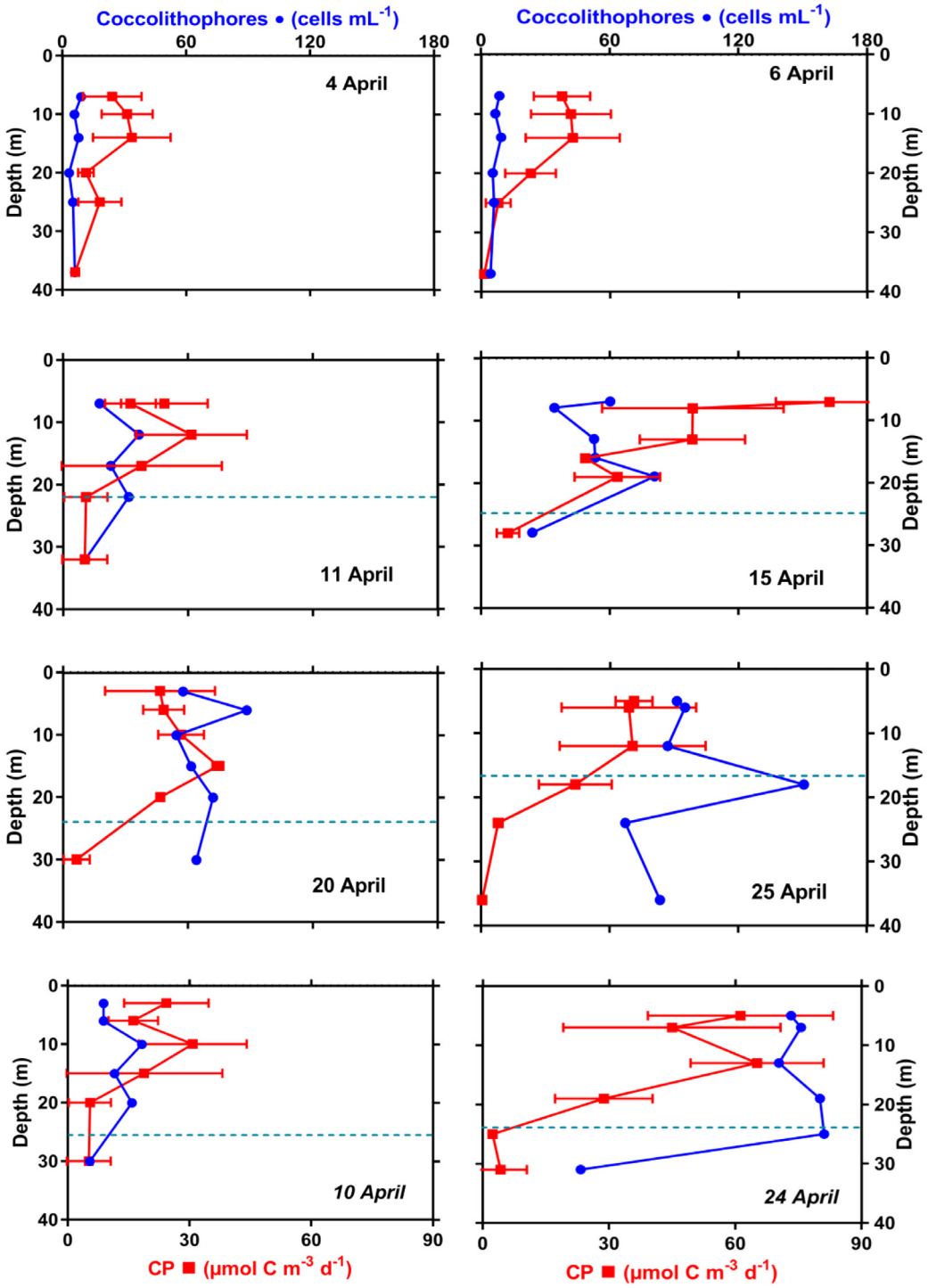

Fig. 3. Vertical profiles of coccolithophore abundance (cells, mL^{-1}) and calcite production (CP, µmol C m^{-3} d^{-1}) over the euphotic zone at the Central Celtic Sea (CCS) and Shelf Edge (CS2 – italicised dates). Dashed line indicates the mixed layer depth.

$cell^{-1}$ (the average content for *E. huxleyi*) (Daniels et al., 2014) coccolithophores generally displayed very low estimated contributions to total chlorophyll-*a* (≤2.4%) along with PP (≤1.3%) (Table 2). The exception to this pattern was station J2 (18.8% and 30.6% contribution to chlorophyll-*a* and PP respectively), which was the site of an *E. huxleyi* bloom (i.e. cell numbers > 1000 mL^{-1}) on April 27th, although this date also had low integrated chlorophyll-*a* (45.2 mg m^{-2}). This may be due to the relatively low chlorophyll-*a* content of *E. huxleyi* cells (0.2–0.34 pg $cell^{-1}$; Daniels et al., 2014; Paasche, 2002). The cruise average PP contribution of coccolithophores (4.1%) agrees well with the low contribution of coccolithophores to PP reported for the north-west European shelf during June 2011 (< 3%; Poulton et al., 2014) and with estimates from other marine environments (see Poulton et al., 2007). This highlights that the biogeochemical importance of coccolithophores during non-bloom conditions does not relate to their organic carbon production (PP), but rather to their inorganic carbon production (CP).

Integrated CP at CCS and CS2 (0.4–1.5 mmol C m^{-2} d^{-1}) was similar to other Celtic sea sites sampled in summer 2011 (0.7–1.2 mmol C m^{-2} d^{-1}; Poulton et al., 2014) suggesting similar spring to summer

Table 3
Averaged euphotic zone and sampled coccolithophore abundance, relative % abundance of E. huxleyi, calcite production (CP) and cell normalised calcification (Cell-CF) for all sites during DY029, Central Celtic Sea (CCS), shelf edge (CS2) and J2 (± represents standard deviation).

Sampling site	Day in April	Coccolithophore abundance (cells mL^{-1})	Growth rate between visits (d^{-1})	Relative abundance of *E. huxleyi* (%)	Relative abundance of *C. caudatus* (%)	Other species (%)	Cell-CF (pmol C $cell^{-1}$ d^{-1})
CCS	04–April	6.3 (± 2)	–	66 (± 12)	5 (± 3)	29 (± 10)	1.7 (± 0.7)
CCS	06–April	6.9 (± 1.9)	0.04 (± 0.02)	53 (± 13)	13 (± 9)	34 (± 5)	1.7 (± 1.1)
CCS	11–April	23.9 (± 10.4)	0.23 (± 0.12)	49 (± 10)	27 (± 7)	24 (± 6)	0.7 (± 0.4)
CCS	15–April	50.9 (± 20)	0.22 (± 0.13)	54 (± 11)	29 (± 5)	17 (± 7)	0.8 (± 0.5)
CCS	20–April	66.4 (± 12.3)	0.05 (± 0.02)	68 (± 7)	26 (± 6)	6 (± 2)	0.4 (± 0.2)
CCS	25–April	95.6 (± 28.5)	0.07 (± 0.02)	76 (± 5)	21 (± 5)	2 (± 1)	0.2 (± 0.2)
CS2	10–April	40.3 (± 11.8)	–	60 (± 2)	10 (± 4)	30 (± 4)	0.9 (± 0.8)
CS2	24–April	134.5 (± 43.9)	0.09 (± 0.04)	56 (± 7)	2 (± 1)	42 (± 8)	0.2 (± 0.2)
J2	14–April	155.6 (–)	–	99 (–)	0	1 (–)	3.4 (–)
J2	27–April	1986.1 (± 42.5)	0.18 (± 0.00)	100 (± 0)	0	0	3.0 (± 0.1)

Table 4
Coccolithophore net growth rates and changes in nitrate concentration (μM d^{-1}) from incubation experiments. Not determined (ND), (± represents standard deviation).

Date in april	Incubation	Coccolithophores (cells ml^{-1})	Growth rate (d^{-1})	ΔNO_3 (μM d^{-1}) (T0 − T48 concentrations)
11	T0	19.2 (± 0.8)	–	ND
	T24	26.2 (± 3.7)	0.31 (± 0.05)	ND
15	T0	53.5 (± 12.1)	–	0.59
	T24	46 (± 17)	−0.15 (± 0.06)	(1.20–0.02)
20	T0	71.9 (± 17.4)	–	1.15
	T24	74.6 (± 4.6)	0.04 (± 0.01)	(2.05–0.02)
25	T0	97.8 (± 35.2)	–	0.20
	T24	118.9 (± 29.7)	0.20 (± 0.09)	(0.41–0.01)
27	T0	2175.9 (± 145.5)	–	0.62
	T24	2431.5 (± 193.8)	0.11 (± 0.01)	(0.65–0.03[a])

[a] Nitrate determined from T24 incubation.

Table 5
Intrinsic growth (k), grazing mortality (g) and net growth rates of coccolithophores for dilution experiments conducted at CCS, CS2 and J2.

Site	Date in April	Growth *k* (d^{-1})	Grazing *g* (d^{-1})	Net growth rate (d^{-1})	R^2
CCS	4	−0.21	0.10	0	0.02
CCS	11	0.86	0.51*	0.35	0.44
CCS	15	0.36	0.60*	−0.36	0.49
CCS	20	−0.39	0.74*	0	0.48
CCS	25	1.23	1.32**	−0.09	0.71
CS2	9	0.41	0.30	0.11	0.20
J2	27	0.29	0.23**	0.06	0.67

* $p < 0.02$.
** $p < 0.002$.

calcification rates. Aside from the coccolithophore bloom on the 27th April at J2, measured ratios of CP to PP (0.01–0.09; Table 2) were also similar to other studies of coccolithophores during non-bloom conditions in shelf regions (0.01–0.11; Poulton et al., 2013, 2014). Within the Iceland Basin in summer these ratios were higher (0.10–0.14; Poulton et al., 2010) suggesting that in open ocean regions CP may represent a greater proportion of fixed carbon than during non-coccolithophore bloom conditions in shelf regions. This is not the case during blooms, such as the one observed at J2 (ratio; 0.46), where CP often represents a large proportion of fixed carbon (~30–40%; Poulton et al., 2007, 2013). The cruise average integrated CP for April 2015 (1.9 ± 3.3 mmol C m^{-2} d^{-1}, excluding the J2 coccolithophore bloom) was similar to the cruise average for a 2011 study around the NW European shelf in summer (2.6 mmol C m^{-2} d^{-1}; Poulton et al., 2014), and slightly lower than in non-bloom conditions in the Iceland Basin (3.6 mmol C $m^{-2}d^{-1}$). Our observed lower rate is likely due to the higher cell numbers (100–870 cells mL^{-1}) observed in the Iceland Basin (Poulton et al., 2010) than in the Celtic Sea in spring (6.3–134.5 cells mL^{-1}).

Integrated CP on the 27th April (240 mmol C m^{-2} d^{-1}) was much greater than observed in other *E. huxleyi* blooms, such as the Iceland Basin (9.5 mmol C m^{-2} d^{-1}), Patagonian Shelf (4 mmol C m^{-2} d^{-1}), or North Sea (11.5 mmol C m^{-2} d^{-1}) (Holligan et al., 1993; Marañón and González, 1997; Poulton et al., 2013). The bloom observed by Poulton et al. (2013) on the Patagonian shelf had lower CP despite high cell numbers (up to 2000 cells mL^{-1}) due to the dominance of the bloom by the low cellular calcite-containing morphotype (morphotype B/C) of *E. huxleyi* (Poulton et al., 2013), whereas morphotype A dominated in the Celtic Sea in April 2015. The A morphotype of *E. huxleyi* has ~50% more coccolith calcite relative to the B/C morphotype (Poulton et al., 2011, 2010), which may have led to the higher CP observed. This is further supported from cell normalised calcification (cell-CF) rates observed on the Patagonian shelf (0.07–0.65 pmol C $cell^{-1}$ d^{-1}) (Poulton et al., 2013) compared to J2 (3 ± 1 pmol C $cell^{-1}$ d^{-1}).

Our observations of coccolithophores during spring suggest at the CCS they occupied a primary biogeochemical role in CP, with only small contributions to phytoplankton biomass (chlorophyll-*a*) or PP. The CP of coccolithophore communities is impacted by the rate at which the populations grow, as well as the composition of the coccolithophore community (Daniels et al., 2016).

4.2. Coccolithophore growth rates in the Celtic Sea

Net growth rates for coccolithophores based on cell abundances between subsequent site visits during our study (0.04–0.25 d^{-1}) were very similar to net growth rates observed from our 24-hour incubation experiments (0.04–0.31 d^{-1}) (Table 4). These results compare well to incubation experiments previously conducted on the north-west European shelf (0.2–0.4 d^{-1}; Poulton et al., 2014), and net growth rates during a spring bloom in the North Atlantic (0.05–0.13 d^{-1}; Daniels et al., 2015). These studies, and our results, also support the observation that coccolithophore populations begin to increase during the spring bloom (Schiebel et al., 2011).

Different species of coccolithophores have been observed to have different net growth rates in culture (Daniels et al., 2014; Gibbs et al., 2013) and natural communities (Daniels et al., 2015, 2016). The net growth rates calculated between site visits for the dominant species in our study (*E. huxleyi* and *C. caudatus*) also differed, with ranges of −0.08 to 0.23 d^{-1} and 0.03 to 0.55 d^{-1}, respectively. Not only the range, but also the timing of maximum growth differed. The maximum net growth period observed for *E. huxleyi* was between 6th–11th April (0.23 d^{-1}) and 11th–15th (0.22d^{-1}), whereas for *C. caudatus* it was 4th–6th April (0.55 d^{-1}). A possible explanation for this temporal

Table 6
Abundance and net growth rates of microzooplankton (ciliates and dinoflagellates) from dilution experiments conducted at CCS, CS2 and J2. Not determined (ND).

Site	Date	Experiment time	Microzooplankton (T0)	Ciliates		Dinoflagellates	
			Cells (L^{-1})	Cells (L^{-1})	Growth rate (d^{-1})	Cells (L^{1})	Growth rate (d^{-1})
CCS	04 April	T0	1610(± 335)	1060 (± 320)	−0.35(± 0.32)	550 (± 100)	0.88(± 0.59)
		T24		750 (± 640)		1330 (± 860)	
	11 April	T0	850(± 355)	470 (± 230)	0.04(± 0.03)	380 (± 270)	−0.34(± 0.31)
		T24		490 (± 220)		270 (± 160)	
	15 April	T0	800(± 255)	300 (± 110)	ND	500 (± 230)	ND
		T24		ND		ND	
	25 April	T0	280(± 160)	140 (± 160)	1.6(± 2.1)	140 (± 0)	1.7(± 0.71)
		T24		690 (± 460)		770 (± 320)	
CS2	09 April	T0	190(± 120)	60 (± 80)	1.58(± 2.35)	130 (± 90)	1.35(± 1)
		T24		290 (± 190)		500 (± 130)	
J2	27 April	T0	460(± 58)	150 (± 50)	0.9(± 0.4)	310 (± 30)	0.95(± 0.29)
		T24		370 (± 110)		800 (± 230)	

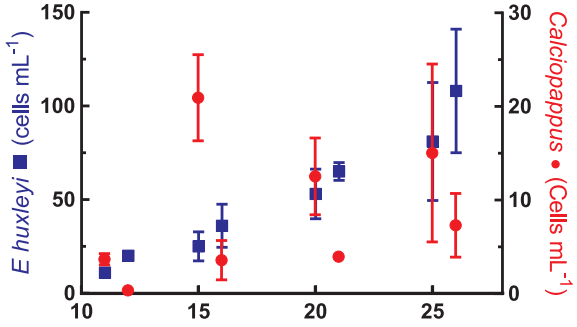

Fig. 4. Cell numbers of *Emiliania huxleyi* (circle) and *Calciopappus caudatus* (squares) from net growth incubation experiments. Lines indicate when separate experiments were conducted.

separation may be that *C. caudatus* is more adapted to the high nutrient-high mixing conditions observed at the beginning of April, a similar high nutrient-low light environment to where it is found in the Arctic Ocean (see Daniels et al., 2016). In contrast, *E. huxleyi* is better adapted to the low nutrient-highly stratified (high light) conditions seen towards late April (Table 1), possibly due to *E. huxleyi*'s ability to utilise different sources of nitrogen and a high affinity for phosphate uptake via alkaline phosphatase (Benner and Passow, 2010; Paasche, 2002). Species-specific growth rates during the incubation experiments were highly variable for *E. huxleyi* (0.21–0.59 d^{-1}) and *C. caudatus* (−0.79 to −2.29 d^{-1}) (Fig. 4). The only noticeable trend being that *E. huxleyi* always showed positive growth, whilst *C. caudatus* often displayed negative growth rates. It is also possible that *C. caudatus* responds negatively to the artificial environment in incubation experiments, which may also explain why it has yet to be maintained in laboratory culture.

Different species of coccolithophores contain different amounts of calcite, based on the number of coccoliths, the calcite content of individual coccoliths and cell size (Daniels et al., 2016; Young and Ziveri, 2000), and the rates of growth (Daniels et al., 2014; Sheward et al., 2017). The amount of cellular calcite within an *E. huxleyi* cell is approximately 0.52 pmol (Poulton et al., 2010; Daniels et al., 2014), whereas for *C.* caudatus it is estimated at ~ 0.09 pmol $cell^{-1}$ (Daniels et al., 2016). Hence, even when *C. caudatus* displayed a higher growth rate than *E. huxleyi* it is unlikely to be the dominant calcifier due to its lower cellular calcite quota and cell abundances than *E. huxleyi* (after Daniels et al., 2014). To determine CP per species it is possible to multiply growth rate, species specific calcite content and species specific abundances (Daniels et al., 2014, 2016). Aside from where negative net growth rates were observed, *C. caudatus* showed a CP_{sp} range of 0.05 to 0.27 pmol C mL^{-1} d^{-1} whilst for *E. huxleyi* this range was 1.34 to 3.8 pmol C mL^{-1} d^{-1}. However, the decline observed in cell-CF throughout April is also likely due to "other" species, such as the larger, and more heavily calcified *Coronosphaera mediterannea* (~9 pmol C $cell^{-1}$ estimated from cell calcite and number of coccoliths per cell; Young and Ziveri, 2000) becoming less abundant (7% contribution to coccolithophore abundance on 4th April and < 1% from 20th April onwards).

Rates of coccolithophore calcification can be impacted by many environmental variables, for example within culture experiments *E. huxleyi* calcification has been shown to increase with increasing nutrient and light stress (Paasche, 2002), particularly under phosphorus limitation (Dyhrman et al., 2006). During nutrient replete conditions, *E. huxleyi* cells have a single layer of coccoliths, whilst during nutrient depletion this is seen to increase to multiple layers (Paasche, 2002; Gibbs et al., 2013). However, nitrate and phosphate concentrations were low at station J2 on 27th April (0.6 and 0.1 μM, respectively), possibly leading to the high rates of calcification. Cells of *E. huxleyi* sampled from this bloom also displayed multiple layers of coccoliths (see Supplementary Figure 1) and a coccolith: cell ratio from SEM images was estimated as ~25 loose coccoliths $cell^{-1}$, further supporting this hypothesis. Detached coccolith:cell ratios have also been used to determine the 'phase' (early, intermediate or late) of coccolithophore blooms, with the ratio increasing over time as the production of coccoliths exceeds rates of cellular division (Poulton et al., 2013). The ratio from the J2 bloom (25 loose coccoliths $cell^{-1}$) suggests sampling activities occurred during the intermediate phase, which appears to be the point of highest calcite production (Poulton et al., 2013). Bloom stage is also likely to be influenced by changing environmental variables, and thus we may have sampled during the time of peak CP. This excess calcification is likely the reason for the high cell-CF values observed at station J2.

Additional information about growth dynamics can be gained from comparing net and potential gross growth rates. Intrinsic (gross) growth rates, measured from dilution experiments, displayed higher values than net growth experiments (0.36–1.23 d^{-1}) (Table 5) which are close to reported estimates for cultured species (0.6–2.8 d^{-1}; Paasche, 2002). By assuming a maximum growth rate of *E. huxleyi* of 1.6 d^{-1}, based on cultures growing in optimum temperature, light and nutrient conditions (Paasche, 2002) we can calculate a growth potential ($u/u_{max} * 100$) for coccolithophores at CCS . The average growth efficiency was ~30% (range: 10–53%) throughout April at CCS, which is very similar to that reported for the Iceland Basin in non-bloom (coccolithophore) conditions (~33%, range 15–54%; Poulton et al., 2010). This suggests that other factors, such as grazers, may be regulating coccolithophore populations in the Celtic Sea.

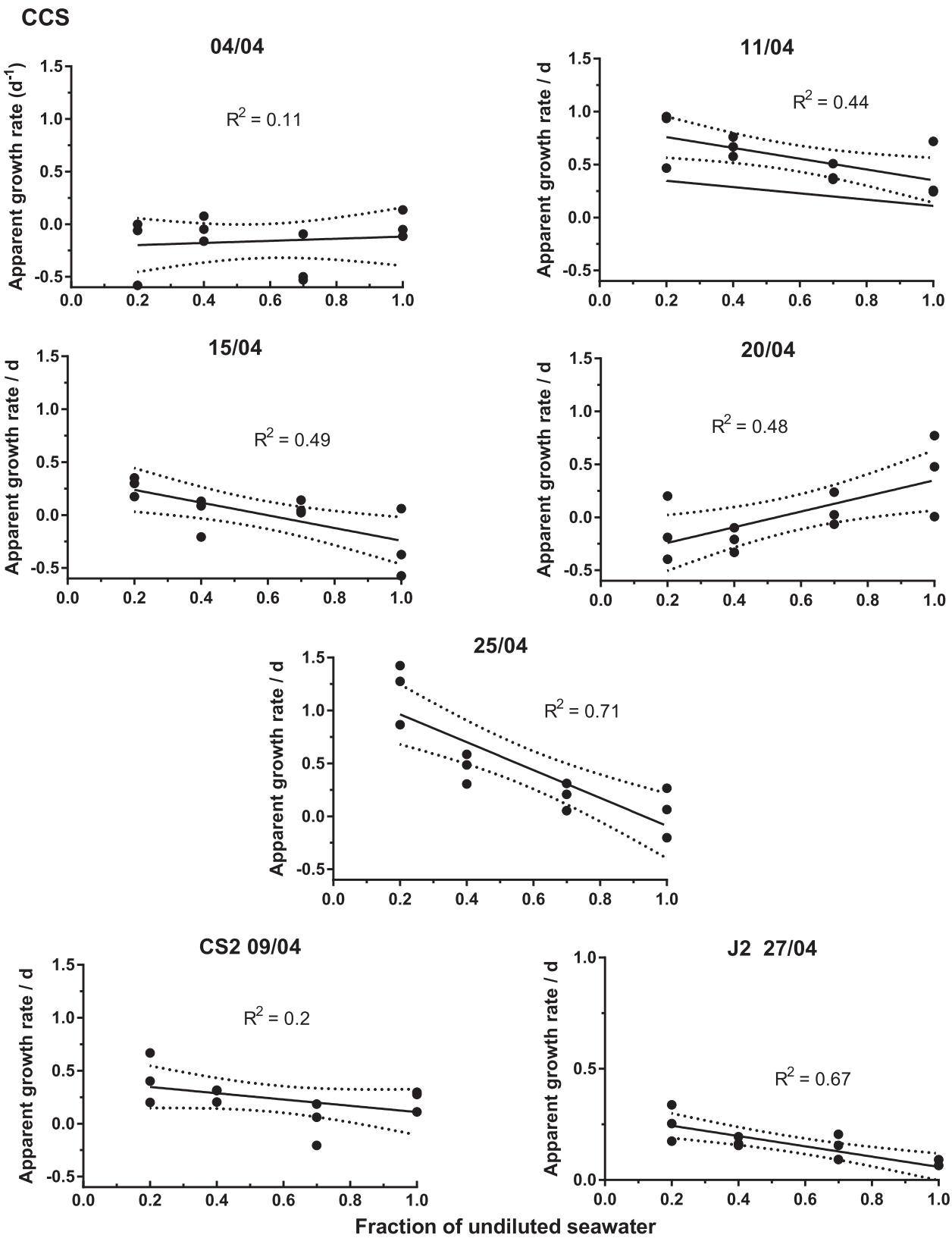

Fig. 5. Plots of the coccolithophore net growth rate (d^{-1}) versus dilution factor from microzooplankton (≤63 μm) grazing experiments from the Central Celtic Sea, Shelf Edge (CS2) and J2 during an *E. huxleyi* bloom.

4.3. Top-down control of coccolithophore populations

Grazing on coccolithophores has previously been demonstrated in laboratory settings (e.g. Hansen et al., 1996; Harvey et al., 2015) and bloom communities in the field (e.g. Archer et al., 2001; Fileman et al., 2002; Holligan et al., 1993; Olson and Strom, 2002), but rarely within non-coccolithophore bloom communities. Moreover, many of the open-ocean mortality rates have been estimated using pigment markers (e.g.

Fileman et al., 2002), flow cytometry (e.g. Archer et al., 2001), and size fractionated chlorophyll (e.g. Olson and Strom, 2002) rather than by direct coccolithophore enumeration by microscopy. In this study, microzooplankton grazing on coccolithophores ranged from 0.10 to 1.32 d^{-1}, which represented a daily consumption of 59 to > 100% of daily calcite production. These values are similar to the range observed from dilution experiments conducted at coastal Atlantic sites for total phytoplankton (35.5–100%) and the global average (65%) of microzooplankton-mediated phytoplankton losses (Schmoker et al., 2013). This suggests a strong top-down control in non-bloom conditions on coccolithophore populations.

A non-significant grazing rate based on the dilution regression was observed at CCS on the 4th April, which was likely to be due to the low coccolithophore cell numbers (at T_0, 100%: 14 cells mL^{-1}; 20%: 4 cells mL^{-1}) encountered (see Supplementary Figure 2). We therefore suggest that this experiment was not able to detect coccolithophore growth or grazing dynamics due to low prey abundances. On the 25th April an "L" shaped curve was seen, suggesting saturated feeding by microzooplankton (Calbet and Saiz, 2013) towards the end of the spring bloom. A polynomial regression was a better fit to the data from 25th April rather than a linear one (R^2 = 0.84 and 0.71 respectively), further supporting a conclusion of a saturated grazer community. This result could also be caused due to alleviation of nutrient limitation via dilution. Hence, the rates observed on this date may be overestimated, though the low net growth rate calculated ($-0.09 d^{-1}$) is lower than the net growth rate incubation observed on this date ($0.07 d^{-1}$), suggesting it may be due to biological differences.

By removing predators over 63 μm in size we are potentially relieving microzooplankton from (meso-zooplankton) grazer control, which would lead to a change in trophic dynamics of the plankton community (Calbet and Saiz, 2013), and potential overestimation of grazing rates in our experiments. A comparison of net growth rates calculated from dilution experiments and net growth rates from incubation experiments (without a pre-treatment of a 63 μm filter) (Tables 3 and 5) shows some differences later in April. These differences imply an increasing importance of complex trophic interactions as the spring bloom progressed (see also Giering et al., this issue), as well as the potential to overestimate grazing rates during late April. Indeed, the biomass of meso-zooplankton (here defined as > 63–500 μm) increased from 1.2 to 1.8 g DW m^{-2} from early to late April (Giering et al., this issue), along with an increasing growth rate, and declining T0 abundance of microzooplankton during late April dilution experiments (Table 6). The trophic positioning of mesozooplankton based on biovolume spectra also displayed an increase from 2.4 to 4.3 from early to late April (Giering et al., this issue). Although it appears we may have induced a trophic cascade, and thus the estimates of grazing from the mid to end of April may be overestimated, grazing rates on coccolithophores (1.32 d^{-1}), were still observed to be very high. This suggest that even if we corrected for these trophic interactions, the grazing rate is still substantial.

The contrast between constant positive accumulation of coccolithophores from subsequent site visits at CCS (Table 3) and the negative rates observed in dilution experiments (Table 5) brings into question the role of mesozooplankton for coccolithophore populations. The observed negative rates from dilution experiments could be due to the release of grazing pressure on microzooplankton and higher mortality rates. However, it also raises the possibility that the presence of mesozooplankton could lead to net accumulation of coccolithophores via a trophic cascade (Calbet and Saiz, 2013). Indeed, mesocosm experiments with added copepods display an increase in autotrophic nanoflagellate communities (Pree et al., 2016; Zöllner et al., 2009), supporting this hypothesis. Although, with no mesozooplankton data from station J2 to compare with we can only speculate on this result for our data. A greater understanding of trophic dynamics within *E. huxleyi* blooms will allow us to test this hypothesis.

Cellular levels of calcite content (i.e. 'calcification state') of *E. huxleyi* cells has been demonstrated to offer no additional protection against microzooplankton grazing in culture experiments (Harvey et al., 2015). In fact, Harvey et al. (2015) observed ingestion rates ~20% higher for calcified *E. huxleyi* cells compared with non-calcified ('naked') cells, although variability in ingestion rates was more strongly linked to the use of different strains. The growth rate of the dinoflagellate prey was also shown to be reduced by ingestion of calcified cells, and was hypothesised to be due to inhibition of food vacuole digestion of the calcite (Harvey et al., 2015). These observations suggest that, particularly for *E. huxleyi*, calcification does not directly provide protection against instantaneous microzooplankton grazing rates, and rather slows the growth rate of the microzooplankton and hence limits their population development (Harvey et al., 2015). During the J2 *E. huxleyi* bloom, growth rates of microzooplankton (0.9 and 0.95 d^{-1} for ciliates and dinoflagellates respectively) compared to CCS on a similar date (1.6 and 1.7 d^{-1}) (Table 6) provides limited support to the suggestion of negative effects of calcite ingestion on microzooplankton grazers. However, these were not the lowest microzooplankton growth rates observed in the Celtic Sea (Table 6), potentially suggesting that other factors (e.g. prey quantity, environmental conditions) may be involved.

The dilution experiment conducted during the *E. huxleyi* bloom at J2 found that a high proportion (~80%) of daily calcite production (0.29 d^{-1}) was grazed (0.23 d^{-1}) (Table 5). The grazing values from J2 in the Celtic Sea in April are higher than other studies during coccolithophore blooms in the Bering Sea (μ, 0.67 d^{-1}; g, 0.14 d^{-1}; Olson and Strom, 2002) and the North Sea (μ, 0.69 d^{-1}; g, 0.36 d^{-1}; Archer et al., 2001), representing losses of 22 and 52% of daily growth, respectively. Both studies observed higher intrinsic growth rates, possibly suggesting these experiments were conducted in an earlier bloom stage to those experienced at J2. Within the Bering Sea bloom, Olson and Strom (2002) measured growth and grazing rates using less than 10 μm chlorophyll-*a* (62 ± 21% of total chlorophyll-*a*). This may have led to an underestimation of rates, particularly as *E. huxleyi* blooms have been shown to contain large chlorophyll-*a* contributions from phytoplankton other than *E. huxleyi* (Poulton et al., 2013; this study). High grazing on *E. huxleyi* has also been observed within the North Atlantic (μ, 0.38 d^{-1}, g, 0.74 d^{-1}; (Holligan et al., 1993), suggesting during periods of *E. huxleyi* blooms microzooplankton can be major agents of mortality. Although large (potentially dsDNA viruses) were detected, viral mortality was not quantified in this *E. huxleyi* bloom. We believe viral mortality to be similar in all dilutions given the size of the virus (~180 nm; Bratbak et al., 1993) and filter size used (0.2 μm).

Both ciliates and dinoflagellates have been observed to graze coccolithophores in culture experiments (Evans and Wilson, 2008; Hansen et al., 1996; Harvey et al., 2015; Kolb and Strom, 2013) suggesting both groups could be responsible for the coccolithophore mortality seen within our study. During *E. huxleyi* blooms ciliates can be a major component of microzooplankton communities (11–51% *Strombidium ovale*; (Archer et al., 2001). However, heterotrophic dinoflagellates can also dominate the microzooplankton biomass within *E. huxleyi* blooms (63% by Gymnodiniales; (Fileman et al., 2002). Throughout an *E. huxleyi* bloom in the Bering Sea, a higher biomass of the large ciliate *Laboea* and the dinoflagellates *Protoperidinium* and *Gyrodinium* were associated with bloom stations (Olson and Strom, 2002). These studies suggest a possible role of microzooplankton composition for *E.* huxleyi populations. A greater understanding of microzooplankton community structure, and the impact of different predators on coccolithophores will help us improve our understanding of coccolithophore bloom dynamics.

We have presented here one of the first set of measurements of microzooplankton grazing (≤63 μm) on coccolithophore populations based on actual cell counts rather than pigment analysis in both coccolithophore bloom and non-bloom conditions. These results indicate that microzooplankton significantly graze coccolithophore populations in shelf seas and exert a strong top-down effect. The results also

question whether calcification is an effective grazer deterrent (e.g. Young, 1994; Monteiro et al., 2016), especially in *E. huxleyi* and microzooplankton dominated communities. This study focused on a shelf sea environment in spring, whilst better understanding of the impact of microzooplankton grazers on coccolithophores requires more measurements from open ocean communities, across seasonal and spatial gradients as well as a direct analysis of grazing rates on coccolithophores by different types of predators.

5. Conclusions

Low contributions (< 2–3%) of coccolithophores towards autotrophic biomass (chlorophyll-a) and primary production during spring in the Celtic Sea implies that coccolithophores have only a minor role in ecosystem dynamics at this time of the year. Rather, the key role for coccolithophores in shelf sea biogeochemistry and carbon cycling is through the production of calcite. Growth rates of coccolithophores varied throughout spring, concurrently with the dynamics of the phytoplankton spring bloom, with generally positive growth rates, particularly for the cosmopolitan *E. huxleyi*. Grazing rates by microzooplankton on coccolithophores were shown to be high (> 60% daily calcite production), suggesting a strong top-down control on coccolithophore populations. This calcite will enter microzooplankton food vacuoles, with pH values during digestion of ~3–5 pH units to ensure the enzymes associated with protist digestion work optimally (Gonzalez et al., 1993; Nagata and Kirchman, 1992). Much of the calcite produced in the euphotic zone could therefore undergo rapid dissolution in microzooplankton food vacuoles, with the resulting carbon respired or excreted. However, calcite could also buffer the pH of the vacuoles and slow the digestion (dissolution) process (Harvey et al., 2015). In this case, microzooplankton growth may be negatively impacted (Harvey et al., 2015), and a portion of the ingested material may be excreted and exported to depth. Clearly, a greater understanding of the pathways for the fate of coccolithophore calcite is required to better understand coccolithophore biogeochemistry and their influence on oceanic CO_2 fluxes.

Acknowledgements

The authors would like to acknowledge the support of the captain, officers and crew of the RRS Discovery as well as all other scientists on board. We would also like to thank the two anonymous reviewers whose comments improved this manuscript. This study was supported by the UK Natural Environmental Research Council via the Shelf Sea Biogeochemistry research programme, via grants NE/K001701/1, NE/K002007/1 and NE/K002058/1. KM was supported by a NERC Doctoral Training Partnership (DTP) studentship as part of the Southampton Partnership for Innovative Training of Future Investigators Researching the Environment (SPITFIRE, grant number NE/L002531/1).

Appendix A. Supplementary material

Supplementary data associated with this article can be found, in the online version, at http://dx.doi.org/10.1016/j.pocean.2018.02.024.

References

Archer, S.D., Widdicombe, C.E., Tarran, G.A., Rees, A.P., Burkill, P.H., 2001. Production and turnover of particulate dimethylsulphoniopropionate during a coccolithophore bloom in the northern North Sea. Aquat. Microb. Ecol. 24, 225–241. http://dx.doi.org/10.3354/ame024225.

Bach, L.T., Larsen, A., Hildebrandt, N., Schulz, K.G., Riebesell, U., 2016. Influence of plankton community structure on the sinking velocity of marine aggregates. Global Biogeochem. Cycles 30, 1145–1165. http://dx.doi.org/10.1002/2015GB005324.

Balch, W.M., Drapeau, D.T., Fritz, J.J., 2000. Monsoonal forcing of calcification in the Arabian Sea. Deep. Res. Part II 47, 1301–1337.

Balch, W.M., 2004. Re-evaluation of the Physiological Ecology of Coccolithophores. In: Thiersten, H.-.R., Young, J.R. (Eds.), Coccolithophores from Molecular Processes to Global Impact. Springer, Berlin.

Balch, W.M., Gordon, H.R., Bowler, B.C., Drapeu, D.T., Booth, E.S., 2005. Calcium carbonate budgets in the surface global ocean based on MODIS data. J. Geophys. Res. Lett. 37, L22605.

Benner, I., Passow, U., 2010. Utilization of organic nutrients by coccolithophores. Mar. Ecol. Prog. Ser. 404, 21–29. http://dx.doi.org/10.3354/meps08474.

Bratbak, G., Egge, J.K., Heldal, M., 1993. Viral mortality of the marine alga Emiliania huxleyi (Haptophyceae) and termination of algal blooms. Mar. Ecol. Prog. Ser. 93, 39–48.

Buitenhuis, E., van Bleijswijk, J., Bakker, D., Veldhuis, M., 1996. Trends in inorganic and organic carbon in a bloom of *Emiliania huxleyi* in the North Sea. Mar. Ecol. Prog. Ser. 143, 271–282. http://dx.doi.org/10.3354/meps143271.

Calbet, A., Saiz, E., 2013. Effects of trophic cascades in dilution grazing experiments: From artificial saturated feeding responses to positive slopes. J. Plankton Res. 35, 1183–1191. http://dx.doi.org/10.1093/plankt/fbt067.

Charalampopoulou, A., Poulton, A.J., Bakker, D.C.E., Lucas, M.I., Stinchcombe, M.C., Tyrrell, T., 2016. Environmental drivers of coccolithophore abundance and calcification across Drake Passage (Southern Ocean). Biogeosciences 13, 5917–5935. http://dx.doi.org/10.5194/bg-13-5917-2016.

Charalampopoulou, A., Poulton, A.J., Tyrrell, T., Lucas, M.I., 2011. Irradiance and pH affect coccolithophore community composition on a transect between the North Sea and the Arctic Ocean. Mar. Ecol. Prog. Ser. 431, 25–43. http://dx.doi.org/10.3354/meps09140.

Daniels, C.J., Poulton, A.J., Esposito, M., Paulsen, M.L., Bellerby, R., St John, M., Martin, A.P., 2015. Phytoplankton dynamics in contrasting early stage North Atlantic spring blooms: composition, succession, and potential drivers. Biogeosciences 12, 2395–2409. http://dx.doi.org/10.5194/bg-12-2395-2015.

Daniels, C.J., Poulton, A.J., Young, J.R., Esposito, M., Humphreys, M.P., Ribas-Ribas, M., Tynan, E., Tyrrell, T., 2016. Species-specific calcite production reveals Coccolithus pelagicus as the key calcifier in the Arctic Ocean. Mar. Ecol. Prog. Ser. 555, 29–47. http://dx.doi.org/10.3354/meps11820.

Daniels, C.J., Sheward, R.M., Poulton, A.J., 2014. Biogeochemical implications of comparative growth rates of Emiliania huxleyi and Coccolithus species. Biogeosciences 11, 6915–6925. http://dx.doi.org/10.5194/bg-11-6915-2014.

Dyhrman, S.T., Haley, S.T., Birkeland, S.R., Wurch, L.L., Cipriano, M.J., Andrew, G., Mcarthur, A.G., 2006. Long serial analysis of gene expression for gene discovery and transcriptome profiling in the widespread marine coccolithophore emiliania huxleyi. Appl. Environ. Microbiol. 72, 252–260. http://dx.doi.org/10.1128/AEM.72.1.252.

Evans, C., Wilson, W.H., 2008. Preferential grazing of oxyrrhis marina on virus-infected emiliania huxleyi. Limnol. Oceanogr. 53, 2035–2040.

Fileman, E.S., Cummings, D.G., Llewellyn, C.A., 2002. Microplankton community structure and the impact of microzooplankton grazing during an Emiliania huxleyi bloom, off the Devon coast. J. Mar. Biol. Assoc. UK 82, 359–368. http://dx.doi.org/10.1017/S0025315402005593.

Frada, M., Young, J., Cachão, M., Lino, S., Martins, A., Narciso, A., Probert, I., de Vargas, C., 2010. A guide to extant coccolithophores (Calcihaptophycidae, Haptophyta) using light microscopy. J. Nannoplankton Res. 31 (2), 58–112.

Gibbs, S.J., Poulton, A.J., Bown, P.R., Daniels, C.J., Hopkins, J., Young, J.R., Jones, H.L., Thiemann, G.J., O'Dea, S.A., Newsam, C., 2013. Species-specific growth response of coccolithophores to Palaeocene-Eocene environmental change. Nat. Geosci. 6, 218–222. http://dx.doi.org/10.1038/ngeo1719.

Giering, S.L.C., Wells, S.R., Mayers, K.M.J., Schuster, H., Cornwell, L., Fileman, E., Atkinson, A., Cook, K.B., Preece, C., Mayor, D.J., 2017. Trophic position of shelf sea zooplankton communities vary in space and time: insights from stable isotope and biovolume spectra analyses. Progress in Oceanography, this issue.

Gifford, D.J., 1988. Impact of grazing by microzooplankton in the Northwest Arm of Halifax Harbour, Nova Scotia. Mar. Ecol. Prog. Ser. 47, 249–258. http://dx.doi.org/10.3354/meps047249.

Gonzalez, J.M., Sherr, B.F., Sherr, E.B., 1993. Digestive enzyme activity as a quantitative measure of protistan grazing: the acid lysozyme assay for bacterivory. Mar. Ecol. Prog. Ser. 100, 197–206. http://dx.doi.org/10.3354/meps100197.

Hansen, F.C., Witte, H.J., Passarge, J., 1996. Grazing in the heterotrophic dinoflagellate Oxyrrhis marina: size selectivity and preference for calcified Emiliania huxleyi cells. Aquat. Microb. Ecol. 10, 307–313. http://dx.doi.org/10.3354/ame010307.

Harvey, E.L., Bidle, K.D., Johnson, M.D., 2015. Consequences of strain variability and calcification in Emiliania huxleyi on microzooplankton grazing. J. Plankton Res. 0, fbv081. doi: 10.1093/plankt/fbv081.

Holligan, P., Viollier, M., Harbour, D., Camus, P., Champagne-Philippe, M., 1983. Satellie and ship studies of coccolithophore production along a continental shelf edge. Lett. Nat. 304, 339–342. http://dx.doi.org/10.1038/304339a0.

Holligan, P.M., Fernández, E., Aiken, J., Balch, W.M., Boyd, P., Burkill, P.H., Finch, M., Groom, S.B., Malin, G., Muller, K., Purdie, D. a., Robinson, C., Trees, C.C., Turner, S. M., van der Wal, P., 1993. A biogeochemical study of the coccolithophore, Emiliania huxleyi, in the North Atlantic. Global Biogeochem. Cycles 7, 879–900. doi: 10.1029/93GB01731.

Hopkins, J., Henson, S.A., Painter, S.C., Tyrrell, T., Poulton, A.J., 2015. Phenological characteristics of global coccolithophore blooms. Global Biogeochem. Cycles 29, 239–253. http://dx.doi.org/10.1002/2014GB004919.

Humphreys, M.P., Achterberg, E.P., Chowdhury, M.Z.H., Griffiths, A.M., Hartman, S.E., Hopkins, J.E., Hull, T., Kivimae, C., Smilenova, A., Wihsgott, J., Woodward, E.M.S., Moore, C.M., 2017. Mechanisms for a nutrient-conserving carbon pump in a seasonally stratified, temperate continental shelf sea. Progress in Oceanography, this issue.

Hydes, D.M., Aoyama, A., Aminot, A., Bakker, K., Becker, S., Coverly, S., Daniels, A., Dickson, A., Grosson, O., Kerouel, R., 2010. Determination of dissolved nutrients (N,

P,Si) in sewater with high precision and inter-comparability using gas segmented continous flow analysers, The GO-SHIP Repeat Hydrography Manual: A collection of export reports and guidelines; IOCCP report No.14, ICPO publication series No.134, version 1.

Iglesias-Rodriguez, M.D., Brown, C.W., Doney, S.C., Kleypas, J.A., Kolber, D., Kolber, Z., Hayes, P.K., Falkowski, P.G., 2002. Representing key phytoplankton functional groups in ocean carbon cycle models: coccolithophorids. Global Biogeochem. Cycles 16http://dx.doi.org/10.1029/2001GB001454. 47-1-47–20.

Klaas, C., Archer, D.E., 2002. Association of sinking organic matter with various types of mineral ballast in the deep sea: implications for the rain ratio. Global Biogeochem. Cycles 16, 1–14. http://dx.doi.org/10.1029/2001GB001765.

Kolb, A., Strom, S., 2013. An inducible antipredatory defense in haploid cells of the marine microalga Emiliania huxleyi (Prymnesiophyceae). Limnol. Oceanogr. 58, 932–944. http://dx.doi.org/10.4319/lo.2013.58.3.0932.

Krueger-Hadfield, S.a., Balestreri, C., Schroeder, J., Highfield, a., Helaouët, P., Allum, J., Moate, R., Lohbeck, K.T., Miller, P.I., Riebesell, U., Reusch, T.B.H., Rickaby, R.E.M., Young, J., Hallegraeff, G., Brownlee, C., Schroeder, D.C., 2014. Genotyping an Emiliania huxleyi (Prymnesiophyceae) bloom event in the North Sea reveals evidence of asexual reproduction. Biogeosciences Discuss. 11, 4359–4408. http://dx.doi.org/10.5194/bgd-11-4359-2014.

Landry, M.R., Hassett, R.P., 1982. Estimating the grazing impact of marine micro-zooplankton. Mar. Biol. 67, 283–288. http://dx.doi.org/10.1007/BF00397668.

Landry, M.R., Kirshtein, J., Constantinou, J., 1995. A refined dilution technique for measuring the community grazing impact of microzooplankton, with experimental tests in the central equatorial Pacific. Mar. Ecol. Prog. Ser. 120, 53–63. http://dx.doi.org/10.3354/meps120053.

Lessard, E.J., Murrell, M.C., 1998. Microzooplankton herbivory and phytoplankton growth in the northwestern Sargasso Sea. Aquat. Microb. Ecol. 16, 173–188. http://dx.doi.org/10.3354/ame016173.

Malin, G., Turner, S., Liss, P., Holligan, P., Harbour, D., 1993. Dimethylsulphide and dimethylsulphoniopropionate in the Northeast atlantic during the summer coccolithophore bloom. Deep. Res. Part I 40, 1487–1508. http://dx.doi.org/10.1016/0967-0637(93)90125-M.

Marañón, E., González, N., 1997. Primary production, calcification and macromolecular synthesis in a bloom of the coccolithophore Emiliania huxleyi in the North Sea. Mar. Ecol. Prog. Ser. 157, 61–77. http://dx.doi.org/10.3354/meps157061.

Monteiro, F.M., Bach, L.T., Brownlee, C., Bown, P., Rickaby, R.E.M., Poulton, A.J., Tyrrell, T., Beaufort, L., Dutkiewicz, S., Gibbs, S., Gutowska, M.A., Lee, R., Riebesell, U., Young, J., Ridgwell, A., 2016. Why marine phytoplankton calcify. Sci. Adv. 2, 1–14. http://dx.doi.org/10.1126/sciadv.1501822.

Nagata, T., Kirchman, D.L., 1992. Release of macromolecular organic complexes by heterotrophic marine flagellates. Mar. Ecol. Prog. Ser. 83, 233–240. http://dx.doi.org/10.3354/meps083233.

Olson, M.B., Strom, S.L., 2002. Phytoplankton growth, microzooplankton herbivory and community structure in the southeast Bering Sea: Insight into the formation and temporal persistence of an Emiliania huxleyi bloom. Deep Res. Part II Top. Stud. Oceanogr. 49, 5969–5990. http://dx.doi.org/10.1016/S0967-0645(02)00329-6.

Paasche, E., Brutak, S., 1994. Enhanced calcification in the coccolithophorid *Emiliania huxleyi* (Haptophycaea) under phosphorus limitation. Phycologia 33, 324–330.

Paasche, E., 2002. A review of the coccolithophorid Emiliania huxleyi (Prymnesiophyceae), with particular reference to growth, coccolith formation, and calcification-photosynthesis interactions. Phycologia 40, 503–529.

Poulton, A.J., Adey, T.R., Balch, W.M., Holligan, P.M., 2007. Relating coccolithophore calcification rates to phytoplankton community dynamics: Regional differences and implications for carbon export. Deep Sea Res Part II Top. Stud. Oceanogr. 54, 538–557. http://dx.doi.org/10.1016/j.dsr2.2006.12.003.

Poulton, A.J., Charalampopoulou, A., Young, J.R., Tarran, G.A., Lucas, M.I., Quartly, G. D., 2010. Coccolithophore dynamics in non-bloom conditions during late summer in the central Iceland Basin (July–August 2007) 55, 1601–1613. doi: 10.4319/lo.2010.55.4.1601.

Poulton, A.J., Painter, S.C., Young, J.R., Bates, N.R., Bowler, B., Drapeau, D., Lyczsckowski, E., Balch, W.M., 2013. The 2008 Emiliania huxleyi bloom along the Patagonian Shelf: ecology, biogeochemistry, and cellular calcification. Global Biogeochem. Cycles 27, 1023–1033. http://dx.doi.org/10.1002/2013GB004641.

Poulton, A.J., Stinchcombe, M.C., Achterberg, E.P., Bakker, D.C.E., Dumousseaud, C., Lawson, H.E., Lee, G.A., Richier, S., Suggett, D.J., Young, J.R., 2014. Coccolithophores on the north-west European shelf: calcification rates and environmental controls. Biogeosciences 11, 3919–3940. http://dx.doi.org/10.5194/bg-11-3919-2014.

Poulton, A.J., Young, J.R., Bates, N.R., Balch, W.M., 2011. Biometry of detached Emiliania huxleyi coccoliths along the Patagonian Shelf. Mar. Ecol. Prog. Ser. 443, 1–17. http://dx.doi.org/10.3354/meps09445.

Poulton, A.J., Davis, C.E., Daniels, C.J., Mayers, K.M.J., Harris, C., Tarran, G.A., Widdicombe, C.E., Woodward, E.M.S., 2017. Seasonal phosphorus and carbon dynamics in a temperate shelf sea (Celtic Sea). Progress in Oceanography, this issue.

Pree, B., Larsen, A., Egge, J.K., Simonelli, P., Madhusoodhanan, R., Tsagaraki, T.M., Våge, S., Erga, S.R., Bratbak, G., Thingstad, T.F., 2016. Dampened copepod-mediated trophic cascades in a microzooplankton-dominated microbial food web: a mesocosm study. Limnol. Oceanogr. 1–14. http://dx.doi.org/10.1002/lno.10483.

Rees, A.P., Woodward, E.M.S., Robinson, C., Cummings, D.G., Tarran, G.A., Joint, I., 2002. Size-fractionated nitrogen uptake and carbon fixation during a developing coccolithophore bloom in the North Sea during June 1999. Deep Res. Part II Top. Stud. Oceanogr. 49, 2905–2927. http://dx.doi.org/10.1016/S0967-0645(02)00063-2.

Richier, S., Achterberg, E.P., Dumousseaud, C., Poulton, A.J., Suggett, D.J., Tyrrell, T., Zubkov, M.V., Moore, C.M., 2014. Carbon cycling and phytoplankton responses within highly-replicated shipboard carbonate chemistry manipulation experiments conducted around Northwest European Shelf Seas. Biogeosci. Discuss. 11, 3489–3534.

Schiebel, R., Brupbacher, U., Schmidtko, S., Nausch, G., Waniek, J.J., Thierstein, H.R., 2011. Spring coccolithophore production and dispersion in the temperate eastern North Atlantic Ocean. J. Geophys. Res. Ocean. 116, 1–12. http://dx.doi.org/10.1029/2010JC006841.

Schmoker, C., Hernandez-Leon, S., Calbet, a., 2013. Microzooplankton grazing in the oceans: impacts, data variability, knowledge gaps and future directions. J. Plankton Res. 35, 691–706. http://dx.doi.org/10.1093/plankt/fbt023.

Sharples, J., Mayor, D.J., Poulton, A.J., Rees, A., Robinson, C., 2017. Preface: Why do shelf seas not run out of nutrients? Progress in Oceanography, this issue.

Sheward, R.M., Poulton, A.J., Gibbs, S.J., Daniels, C.J., Bown, P.R., 2017. Physiology regulates the relationship between coccosphere geometry and growth phase in coccolithophores. Biogeosciences 14 (6), 1493–1509.

Smyth, T.J., Tyrell, T., Tarrant, B., 2004. Time series of coccolithophore activity in the Barents Sea, from twenty years of satellite imagery. Geophys. Res. Lett. 31, 2–5. http://dx.doi.org/10.1029/2004GL019735.

Taylor, J.R., 1982. An introduction to Error Analysis. University Science Books, Sausalito, California, pp. 327.

Tyrrell, T., Merico, A., 2004. Emiliania huxleyi bloom observations and the conditions that induce them. In: Thiersten, H.-R., Young, J.R. (Eds). Coccolithophores from Molecular Processes to Global Impact, Springer, Berlin.

Winter, A., Siesser, W.G., 1994. Atlas of Living Coccolithophores. In: Winter, A., Siesser, W.G. (Eds.), Coccolithophores. Cambridge University Press, Cambridge, pp. 107–159.

Woodward, E.M.S., Rees, A., 2001. Nutrient distributions in an anticyclonic eddy in the northeast Atlantic Ocean, with reference to nanomolar ammonium concentrations. Deep Res. Part II 48 (4), 775–793.

Young, J.R., 1994. Function of Coccoliths. In: Winter, A., Siesser, W.G. (Eds.), Coccolithophores. Cambridge University Press, Cambridge, pp. 63–82.

Young, J.R., Geisen, M., Cros, L., Kleijne, a., Sprengel, C., Probert, I., Østergaard, J., 2003. A guide to extant coccolithophore taxonomy. J. Nannoplankt. Res. 125.

Young, J.R., Ziveri, P., 2000. Calculation of coccolith volume and its use in calibration of carbonate flux estimates. Deep Res. Part II Top. Stud. Oceanogr. 47, 1679–1700. http://dx.doi.org/10.1016/S0967-0645(00)00003-5.

Ziveri, P., de Bernardi, B., Baumann, K.H., Stoll, H.M., Mortyn, P.G., 2007. Sinking of coccolith carbonate and potential contribution to organic carbon ballasting in the deep ocean. Deep. Res. Part II 54, 659–675. http://dx.doi.org/10.1016/j.dsr2.2007.01.006.

Zöllner, E., Hoppe, H.-G., Sommer, U., Jürgens, K., 2009. Effect of zooplankton-mediated trophic cascades on marine microbial food web components (bacteria, nanoflagellates, ciliates). Limnol. Oceanogr. 54, 262–275. http://dx.doi.org/10.4319/lo.2009.54.1.0262.